applied sciences

MDPI

Article

Water Resistant Composite Membranes for Carbon Dioxide Separation from Methane

Colin A. Scholes

Department of Chemical Engineering, The University of Melbourne, Melbourne, VIC 3010, Australia; cascho@unimelb.edu.au; Tel.: +61-3-9035-8289

Received: 17 April 2018; Accepted: 17 May 2018; Published: 21 May 2018

Abstract: Membranes that are resistant to water vapor permeation have potential in natural gas sweetening by reducing the need for pretreatment. The perfluorinated polymer Teflon AF1600 has proven resistance to water vapor, which is adapted here in the form of composite membranes consisting of a Teflon AF1600 protective layer on membranes of the polyimide 4,4′-(hexafluoroisopropylidene) diphthalic anhydride 2,3,5,6-tetramethyl-1,4-phenylenediamine (6FDA-TMPDA) as well as Polymer of Intrinsic Micro-porosity (PIM-1). The permeability of CO_2 and CH_4 through the composite membranes was shown to be a function of the respective permeabilities of the individual polymer layers, with the Teflon AF1600 layer providing the majority of the resistance to mass transfer. Upon exposure to water, the composite membranes had reduced water permeation of 7–13% compared to pure membranes of 6FDA-TMPDA and PIM-1, because of the water resistance of the Teflon AF1600 layer. It was observed that water permeated as clusters through the composite structure. Under CO_2-CH_4 mixed gas conditions, 6FDA-TMPDA layer permselectivity performance was reduced and became comparable to Teflon AF1600, while the PIM-1 layer retained much of its high permselectivity performance. Importantly, at water activities below 0.2 the PIM-1 composite membrane achieved higher permeability for CO_2 compared to water.

Keywords: composite membranes; Teflon AF1600; PIM-1; polyimide; water; CO_2/CH_4 separation

1. Introduction

Gas separation polymeric membranes that are resilient to water permeance have important application in the natural gas sweetening industry [1–3]. This is due to trace water content within natural gas, which is known to reduce membrane separation performance because of competitive sorption and plasticization [4]. Currently, most natural gas sweetening processes involving membranes require extensive pretreatment to remove water vapor and protect the membrane, which is generally through a glycol dehydration process. This also creates a problem in that glycol vapor entrained in the natural gas will also reduce the separation performance of downstream polymeric membranes [5]. Previous research has demonstrated that exposure to water vapor can reduce the permselectivity of the polyimide 6FDA-TMPDA by 50% [6] and for high performance PIM-1 membranes by 38% [7]. The majority of the research has focused on water removal from the feed stream, in dehydration applications [8–14]. In contrast, perfluorinated polymers Teflon AF1600 and Hyflon AD60 membranes demonstrate significant resistance to separation performance loss in the presence of water vapor [15]. Interestingly, under certain conditions Teflon AF1600 has selectivity for CO_2 over H_2O, which has not been observed in any other polymeric membranes [4]. However, perfluroinated polymers are expensive compared to current commercial polymeric membranes and have only average permselectivity for CO_2 against CH_4. Hence, polymeric membranes based exclusively on perfluorinated polymers are not viable. Instead, utilizing the perfluorinated polymers as a non-porous protective layer in a composite membrane strategy is a more feasible approach, with the perfluorinated polymer

limiting water permeance while the majority of separation of CO_2 from CH_4 is undertaken by a high performing polymer.

Here, composite membranes consisting of the perfluorinated polymer Teflon AF1600 coated on the polyimide 6FDA-TMPDA or Polymer of Intrinsic Microscopy (PIM-1) are investigated for their CO_2 separation from CH_4 performance, under mixed gas conditions in the presence of water vapor. The purpose is to overcome both the polyimide and PIM-1 susceptibility to water vapors through the protection provided by the perfluorinated polymer's non-porous layer. In particular, the composite membranes perfluorinated polymer layer thickness is varied to determine how much resistance is provided by that layer, and how this impacts the composite membranes' separation performance.

For a composite membrane, the flux of a gas A (J_A) through the overall membrane follows the solution–diffusion mechanism and can be determined by [16]:

$$J_A = \left(\frac{P_A}{l}\right)\Delta f = \frac{\Delta f}{R_T} \quad (1)$$

where P_A is the overall composite membrane permeability of gas A, Δf is the fugacity difference across the membrane and l is the membrane thickness. The permeability divided by the thickness is the membrane permeance, which can also be expressed in terms of total resistance to mass transfer (R_T). For a composite membrane, the total resistance can be expressed as the sum of the resistances from the feed side boundary layer (R_F), the permeate side boundary layer (R_P), and the membrane layers (R_{L1} and R_{L2}) [17]:

$$R_T = R_F + R_P + R_{L1} + R_{L2} \quad (2)$$

The boundary layer resistances on the feed and permeate sides (R_F and R_P) arise from concentration polarization. For a single gas permeation measurement, there is no concentration polarization on either the feed or permeate sides, and hence the total resistance to flow is related to only to the respective thickness of the different layers and their respective permeabilities:

$$R_T = R_{L1} + R_{L2} = \frac{l_{L1}}{P_{L1}} + \frac{l_{L2}}{P_{L2}} \quad (3)$$

Hence, the resistance and the permeability of the composite membrane can be determined based on the permeabilities and thicknesses of the respective layers. Under mixed gas conditions, concentration polarization can be avoided on the feed and permeate sides of the membrane if operated at low stage cuts, and hence the resistance and permeability of the composite membrane can be determined from the performance of the individual layers of the composite structure.

The permeability of the gas through a glassy polymeric membrane can be described through the solution–diffusion mechanism, which explains the transport by diffusion-solubility through the membrane. The sorption (S_A) of a gas within the polymeric membranes to the polymeric matrix through Henry's Law and to the micro-voids within the glassy polymeric structure as Langmuir adsorption [16]:

$$S_A = k_{DA} + \frac{C'_{HA} b_A}{(1 + b_A f_A)} \quad (4)$$

where k_{DA} is the Henry's law constant, C'_{HA} the maximum adsorption capacity and b_A the Langmuir affinity constant. The diffusion of gas species adsorbed in the micro-void region is partially immobilized. To account for this a parameter F_A is introduced to describe the fraction of penetrant in the micro-void region that is mobile [18]:

$$S_A = k_{DA} + \frac{F_A C'_{HA} b_A}{(1 + b_A f_A)} \quad (5)$$

When binary gases are present the competitive sorption occurs in the micro-void region and the solubility of gas A is reduced. Hence, the mobile solubility of gas A in the membrane becomes [19]:

$$S_A = k_{DA} + \frac{F_A C'_{HA} b_A}{(1 + b_A f_A + b_B f_B)} \quad (6)$$

where b_B is the Langmuir affinity constant of the competing gas B. The corresponding average permeability for gas A (P_A) through the membrane can therefore be calculated by the integration of the diffusivity and solubility at the feed (f_{A0}) and permeate (f_{A1}) sides of the membrane, where D_A is the diffusivity of gas A:

$$P_A = \int_{f_{A0}}^{f_{A1}} D_A \,.\, S_A \, df \quad (7)$$

2. Experimental Section

Amorphous Teflon AF1600 (copolymer of 65 mol% 2,2-bis-trifluoromethyl-4,5-difluoro-1,3-dioxode and 35 mol% tetrafluoroethylene) was purchased from DuPont (Houston, TX, USA). The polyimide 6FDA-TMPDA was synthesized by the reaction between 4,4′-(hexafluoroisopropylidene) diphthalic anhydride and 2,3,5,6-tetramethyl-1,4-phenylenediamine in n-methylpyrolidone (AR grade) under Ar to give the polyamic acid, which was subsequently imidized with trimethylamine and acetic anhydride to yield 6FDA-TMPDA. Details of the synthesis can be found elsewhere [20]. PIM-1 was the polycondensation product of monomers 5,5′,6,6′-tetrahydroxy-3,3,3′,3′-tetramethyl-1,1′-spirobisindane (TTSBI) and 2,3,5,6-tetrafluoroterephthalonitrile (TFTPN) and synthesized following established procedures by Budd et al. [21].

The dense 6FDA-TMPDA and PIM-1 layers were prepared by controlled evaporation of a 2.5 w/v % solution from dichloromethane. Evaporation was achieved by partially sealing the solution from the atmosphere so that the dichloromethane partial pressure above the film surface was high, preventing rapid solvent loss. This procedure produced membranes of 6FDA-TMPDA with a thickness of 42 µm and membranes of PIM-1 with a thickness of 35 µm. The perfluorinated polymer layer was spin coated from a 2 w/v % solution (fluorinated solvent PF5060 (3M, Melbourne, Australia)) on top of the 6FDA-TMPDA and PIM-1 films for various thicknesses (Table 1). The different solvation properties of 6FDA-TMPDA and PIM-1 compared to Teflon AF1600 means that there was no redissolving of the underlying polymer layer when the perfluoropolymer film was applied. All films were annealed under vacuum at 40 °C for 3 days. To minimize any age dependent behavior, all membranes were used within 4 days of annealing. This annealing temperature is lower than that which is common for the polyimide 6FDA-TMPDA and PIM-1, and was used to ensure that the perfluorianted polymer did not undergo thermal degradation during the annealing process. The unique surface properties of Teflon AF1600 meant that it formed a discrete layer on top of the 6FDA-TMPDA and PIM-1 membranes which could be peeled off the underlying membrane under the correct shear conditions. Hence, there was a distinct boundary between the two layers. Furthermore, the thickness of the Teflon AF1600 layer was dictated by the needed to form a uniformed film on the membrane, as lower amount of perfluorinated polymer do not form a consistent membrane.

Table 1. Total thickness (µm) of composite PIM-1 and 6FDA-TMPDA membranes with various thickness of the Teflon AF1600 protective layer.

Selective Layer	Selective Layer Thickness (µm)	Teflon AF1600 Thickness	Total Composite Thickness (µm)
6FDA-TMPDA	42 ± 0.5	6 ± 0.5	48 ± 1
6FDA-TMPDA	42 ± 0.5	8 ± 0.5	50 ± 1
6FDA-TMPDA	42 ± 0.5	12 ± 0.5	54 ± 1
PIM-1	35 ± 0.5	5 ± 0.5	40 ± 1
PIM-1	35 ± 0.5	8 ± 0.5	43 ± 1
PIM-1	35 ± 0.5	10 ± 0.5	45 ± 1

Single gas permeabilities were undertaken on a variable pressure constant volume apparatus that has previously been reported [22]. Single gas measurements were undertaken with a feed pressure of 0.987 atm at 35 °C. Mixed gas permeability measurements were undertaken on a constant pressure variable volume instrument, which has also been previously reported and the protocol for exposure to water vapor has also been previously reported [6]. The feed gas was 10% CO_2 in CH_4 mixture at 9.87 atm and 35 °C. The choice in single gas and mixed gas feed pressures were to ensure the membranes experience the same partial pressure of CO_2 under both single and mixed gas conditions. Vapor concentration polarization was not an issue for these polymeric membrane systems because of the low stage cut (<0.1), but to ensure good flow conditions the feed flowrate was at 100 mL/min and the helium sweep gas was at 24 mL/min, which are comparable to previous mixed gas with vapor studies [7]. Pure CO_2 (99.5% Industrial grade), pure CH_4 (99.9% High purity) and 10% CO_2 in CH_4 mixed gas where obtained from Coregas (Melbourne, Australia). Gas permeate flowrate was measured through a universal flowmeter (Agilent Technologies ADM3000) and composition through gas chromatography (Varian CP-3800, with Molecular sieve and PORAPAK Q columns). Humidity of the wet gas feed and permeate streams were measured through a humidity transmitter (HMT, Probe type 334 Vaisala Oyj, Helsinki, Finland).

3. Results and Discussion

3.1. Hydrophobicity of the Composite Membranes

The hydrophobicity of the composite membranes is demonstrated by water contact angles on the surface, provided in Table 2 along with that of pure Teflon AF1600 film. The contact angle observed for pure Teflon AF1600 is comparable with literature and highlights the superhydrophobic surface of the perfluoropolymer [23]. The composite membranes all have comparable water contact angles to that of the pure Teflon AF1600 layer, demonstrating that the superhydrophobic layer covers the composite structure surface. In contrast, PIM-1 has a reported water contact angle of 85° [24], while the 6FDA-TMPDA film had a measured contact angle of 88°. While these contact angles correspond to hydrophobic materials, that are not to the same degree as that of Teflon AF1600, and hence the perfluoropolymer layer will hinder water transport through the composite membrane structure.

Table 2. Advancing water contact angle (degree) on the composite PIM-1 and 6FDA-TMPDA membranes with various thickness of the Teflon AF1600 protective layer, as well as that of pure Teflon AF1600.

Selective Layer	Total Composite Thickness (μm)	Advancing Contact Angle (degs)
Pure Teflon AF1600	8 ± 0.5	128.3 ± 0.2
6FDA-TMPDA	48 ± 1	124.3 ± 0.8
6FDA-TMPDA	50 ± 1	124.2 ± 0.8
6FDA-TMPDA	54 ± 1	124.7 ± 0.7
PIM-1	40 ± 1	126.3 ± 0.5
PIM-1	43 ± 1	126.2 ± 0.4
PIM-1	45 ± 1	126.5 ± 0.6

3.2. Single Gas Permeability

The single gas permeability of CO_2 and CH_4 through the pure 6FDA-TMPDA, PIM-1 and Teflon AF1600 membranes are provided in Table 3 at 35 °C. Additionally included in the table is permeability of H_2O under mixed gas conditions, where the carrier gas is N_2 at 4 bar, 35 °C, and 0.3 water activity. The 6FDA-TMPDA membrane permeabilities are comparable to literature [22,25], given the differences in annealing temperature, and clearly demonstrate the high water permeance and corresponding large water selectivity relative to CO_2. PIM-1 permeabilities are higher than the majority of the literature [21,26,27]. This difference is attributed to the low feed pressure, meaning the micro-voids are not saturated and hence the CO_2 solubility is greater than that observed for other studies undertaken

at higher pressures [28]. The water permeability through PIM-1 is comparable to the author's previous study [7], and demonstrates that PIM-1 has selectivity for water over CO_2. The Teflon AF1600 permeabilities are comparable with literature [15] and demonstrate the unique selectivity for CO_2 over H_2O. The low permeability of water in Teflon AF1600 is associated with the super-hydrophobicity of the polymer and the observation of very low water sorption into the Teflon AF1600 membrane structure. It has been hypothesized that water vapor transports through the perfluoropolymer in the form of clusters, because of the super-hydrophobocity of the polymer chains. The formation and size of the water clusters reduces the diffusivity of water vapor, which when coupled with the very low water solubility results in low water permeability.

Table 3. Single gas permeability (barrer) in pure 6FDA-TMPDA, PIM-1 and Teflon AF1600 membranes, at 35 °C.

Membrane	CO_2	CH_4	H_2O	CO_2/CH_4	H_2O/CO_2
6FDA-TMPDA	605 ± 11	46 ± 2	22600 ± 550	13.2	37.2
PIM-1	5613 ± 23	355 ± 6	25200 ± 700	15.8	4.5
Teflon AF1600	527 ± 18	40.5 ± 1.8	425 ± 40	13.0	0.8

Modelling of the CO_2 permeability through Equations (5) and (7) enables the interconnection between the micro-voids within the membranes to be determined. This is achieved by calculating the mobility factor (F_A), and indication of the proportion of gas diffusing through the micro-voids that can transverse through the entire membrane. The other fundamental parameters of the three pure membranes have already been reported in the literature and are provided in Table 4. The calculated mobility factor for Teflon AF1600 is comparable to literature, but that of 6FDA-TMPDA and PIM-1 are lower than that reported in the literature [7,15,25]. This implies that the 6FDA-TMPDA and PIM-1 membranes studied here have reduced interconnectivity between the micro-voids, which is attributed to the annealing temperature of the membranes. The lower temperature limits chain rearrangement during the annealing process and has restricted interconnectivity between the micro-voids.

Table 4. CO_2 permeability and competitive sorption parameters for 6FDA-TMPDA, PIM-1 and Teflon AF1600, taken from the literature. The F values are calculated from the data, with those values in brackets corresponding to literature.

Membrane	D (cm^2/s)	k_D (cm^3/cm^3 atm)	C'_H (cm^3/cm^3)	b (atm^{-1})	F
6FDA-TMPDA [25]	6.5×10^{-7}	3.2	59	0.55	0.18 (0.57)
PIM-1 [7]	5.5×10^{-6}	1.3	57	0.52	0.33 (0.9)
Teflon AF1600 [15]	2.9×10^{-6}	1.22	15.4	0.10	0.12 (0.17)

The single gas permeabilities of CO_2 and CH_4 through the composite membranes are provided in Table 5 at 35 °C; arranged by polymer type and thickness of the perfluorinated layer. It is clear that all six composite membranes have CO_2 permeability greater than CH_4, and therefore have potential for the separation of CO_2 from natural gas. The composite membranes with a PIM-1 layer have CO_2 permeabilities on the order of 1803–2547 barrer, which are over three times that observed for those composite membranes with a 6FDA-TMPDA layer, 607–640 barrer. This is attributed to the different permeability through the polyimide and PIM-1 layers respectively, rather than the perfluorinated layer, as this layer is expected to have similar CO_2 permeability irrespective of the composite membrane. The CO_2 permeability decreases through the composite membranes as the thickness of the membrane increases, which corresponds to a thicker Teflon AF1600 layer. This reveals that the Teflon AF1600 layer is hindering gas permeance relative to the PIM-1 or 6FDA-TMPDA layers; which is anticipated from the lower single gas permeabilities through the individual Teflon AF1600 membrane (Table 3).

There is little change in the CO_2/CH_4 selectivities of the two composite membranes as a function of thickness, as the results are within error of each other for the two composite membrane series.

Table 5. Single gas CO_2 and CH_4 permeabilities (barrer) through 6FDA-TMPDA and PIM-1 composite membranes with Teflon AF1600, denoted by overall membrane thickness, at 35 °C.

Membrane	Thickness (μm)	CO_2	CH_4	CO_2/CH_4
6FDA-TMPDA	48	640 ± 10	47.6 ± 2	13.5
6FDA-TMPDA	50	617 ± 14	48.3 ± 4	12.8
6FDA-TMPDA	54	607 ± 13	47.4 ± 4	12.8
PIM-1	40	2547 ± 38	181 ± 6	14.1
PIM-1	43	2007 ± 41	144 ± 6	14.0
PIM-1	45	1803 ± 36	131 ± 6	13.8

Assuming the perfluorinated polymer layers in the composite membranes have the same CO_2 and CH_4 permeabilities as pure membranes of the polymers (Table 3), then the respective average permeabilities of the 6FDA-TMPDA and PIM-1 layers can be determined through Equation (3), and are provided in Table 6. This assumption is valid because of the poor solvation properties of the Teflon AF1600 polymer, meaning it does not integrate, blend or be modified by the underlying 6FDA-TMPDA or PIM-1 layer structure. The composite membranes all have higher CO_2 and CH_4 permeability for the 6FDA-TMPDA and PIM-1 layers than the pure membranes of these polymers. For 6FDA-TMPDA there is an increase in 7%, which suggests a more open morphology in the composite membrane compared to the pure membrane, but given the similarly with the error of the measurement this cannot be definitively concluded. The corresponding CO_2/CH_4 selectivity of the 6FDA-TMPDA and PIM-1 layers in the composite membranes are comparable to the individual membranes of these polymers, revealing that the difference between the composite structure and individual membranes impacts CO_2 and CH_4 equally.

Table 6. Calculated permeabilities (barrer) through composite membranes' 6FDA-TMPDA and PIM-1 layers.

Membrane	CO_2	CH_4	CO_2/CH_4
6FDA-TMPDA layer	645 ± 12	49.6 ± 1	13.0
PIM-1 layer	5697 ± 60	354 ± 9	16.1

The water permeability through the composite membranes is provided in Table 7, at a water activity of 0.3, and clearly demonstrates a dramatic decrease relative to that observed for the pure 6FDA-TMPDA and PIM-1 membranes (Table 3). Indeed, all six composite membranes have comparable water permeability indicative that the Teflon AF1600 layer is acting as a protective film and reducing the water transport through the composite membrane structures. For both 6FDA-TMPDA and PIM-1 composite membranes, increasing the thickness of the Teflon AF1600 layer reduces the corresponding water permeability, supporting the conclusion that the perfluoropolymer layer restricts water transport through the membrane. The corresponding H_2O/CO_2 selectivity of the composite membranes are reduced relative to the pure membranes (Table 3), and for the PIM-1 composite membranes the H_2O/CO_2 selectivity is essentially unity. Hence, there is no selectivity for water. This is an important finding and demonstrates that the perfluoropolymer in a composite structure achieves water resistant polymeric membranes with reasonable permselectivity for gas separation.

Table 7. H_2O permeability (barrer) and H_2O/CO_2 selectivity through 6FDA-TMPDA and PIM-1 composite membranes with Teflon AF1600, denoted by overall membrane thickness, at 35 °C.

Membrane	Thickness (μm)	H_2O	H_2O/CO_2
6FDA-TMPDA	48	2810 ± 120	4.4
6FDA-TMPDA	50	2300 ± 120	3.7
6FDA-TMPDA	54	1740 ± 130	2.9
PIM-1	40	2900 ± 100	1.1
PIM-1	43	2050 ± 120	1.0
PIM-1	45	1760 ± 120	0.98

The water permeability through the 6FDA-TMPDA and PIM-1 layers of the composite membranes can be calculated from Equation (3), if it is assumed that the water permeability through the Teflon AF1600 layer is equal to that of the individual membrane (Table 3). The average calculated water permeability is provided in Table 8. These permeabilities are clearly reduced compared to that of the pure polymeric membranes. For 6FDA-TMPDA, H_2O permeability has been reduced by 35% and for PIM-1, H_2O permeability has been reduced by 33%. These decreases are significant and beyond error associated with experimentation. A likely explanation for this behavior is a change in the mode in which water vapor is transporting through the 6FDA-TMPDA and PIM-1 layers, due to the composite structure. The water cluster that is hypothesized to transverse the Teflon AF1600 layer is likely being partly retained within the 6FDA-TMPDA and PIM-1 layers, lowering diffusivity and hence reducing the corresponding water permeability. This can be demonstrated through Graham's Law of Diffusion, which relates diffusivity ratio to molecular weight ratio [29]:

$$\frac{D_1}{D_2} = \sqrt{\frac{M_2}{M_1}} \tag{8}$$

Table 8. Calculated water permeability (barrer) through composite membranes' 6FDA-TMPDA and PIM-1 layers.

Membrane	H_2O
6FDA-TMPDA layer	14590 ± 350
PIM-1 layer	16920 ± 600

Accounting for competitive sorption effects in the permeability, the diffusivity of water in the pure and composite membranes of 6FDA-TMPDA and PIM-1 can be calculated. The diffusivity ratio for composite and pure PIM-1 membranes correspond to a molecular weight ratio of 2.2:1 (composite to pure membrane), and for 6FDA-TMPA the molecular weight ratio is 2.4:1. This reveals that within the composite membrane water is diffusing through the PIM-1 and 6FDA-TMPDA as clusters of twice the size or more of water diffusing through pure membranes of these polymers. Hence, the perfluoropolymer layer acts as a barrier to water vapor transport and also reduces water transport through the selective layer. This mechanism for water permeation through the membranes is graphically depicted in Figure 1.

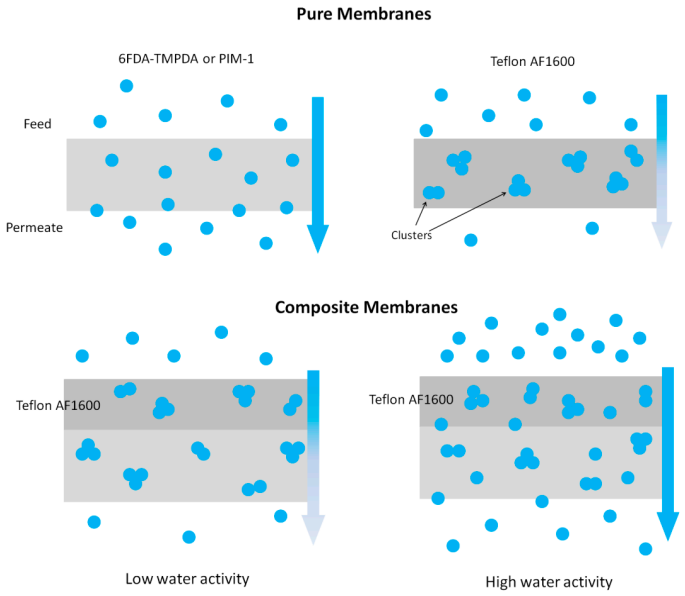

Figure 1. Schematic of water transport through the respective individual and composite membranes.

3.3. Mixed Gas Permeability

The mixed gas permeabilities of the individual membranes of 6FDA-TMPDA, PIM-1 and Teflon AF1600 are provided in Table 9 for a 10% CO_2 in CH_4 feed gas. For all three membranes the CO_2 and CH_4 permeabilities are reduced relative to the single gas feeds, expect for Teflon AF1600 CH_4 permeability which is within error of the single gas measurement. This reduction in permeability is associated with competitive sorption between the two gases present reducing the solubility of each gas within the membrane structure. The change in CO_2/CH_4 selectivity varies, for PIM-1 and Teflon AF1600 the selectivity reduces and indicates that CO_2 sorption is more impacted by CH_4. Contrasting to this, 6FDA-TMPDA membrane selectivity is increased under mixed gas conditions, implying that CH_4 sorption is more strongly impacted by CO_2, than the other way. This behavior is associated with both the membrane morphology and the affinity each gas has for the micro-voids of the three polymeric membranes [19]. Interestingly, under mixed gas conditions Teflon AF1600 has a greater CO_2 permeability than 6FDA-TMPDA, which differs from the single gas result, and implies in the composite membranes the 6FDA-TMPDA layer will hinder gas permeance more than the perfluoropolymer. The reduction in CO_2 permeability under mixed gas conditions can be modelled through competitive sorption theory (Equations (6) and (7)), with the Langmuir affinity constant of CH_4 the only variable, given the established parameters for the three polymers already supplied in Table 4. Hence, the determined Langmuir affinity constants are provided in Table 9. The affinity constant for Teflon AF1600 and 6FDA-TMPDA closely align with those previously reported in the literature [15,22], while to the best of the author's knowledge no CH_4 affinity constant has previously been reported for PIM-1. The CH_4 affinity constants for 6FDA-TMPDA and PIM-1 are considerably less than that of CO_2, which is associated with the strong affinity CO_2 has for those two polymers; while for Teflon AF1600 the affinity constants for CO_2 and CH_4 are comparable, which is associated with the poor affinity Teflon AF1600 has for many gases and vapors.

Table 9. Mixed gas permeability (barrer) in pure 6FDA-TMPDA, PIM-1 and Teflon AF1600 membranes, at 35 °C.

Membrane	CO_2	CH_4	CO_2/CH_4	b_{CH4} (atm^{-1})
6FDA-TMPDA	477 ± 32	20.9 ± 3	22.4	0.11
PIM-1	3350 ± 220	288 ± 21	12.5	0.16
Teflon AF1600	485 ± 36	42.1 ± 8	11.5	0.07

The mixed gas permeabilities of the composite membranes are provided in Table 10 for a 10% CO_2 in CH_4 feed gas. For the 6FDA-TMPDA composite membranes, the CO_2 permeability is within error of the individual Teflon AF1600 and 6FDA-TMPDA membranes, while the CH_4 permeability is similar to that of the 6FDA-TMPDA membrane. From the pure membrane measurements both polymers have similar permselectivity and hence the composite structure achieves no enhancement over the individual polymers. In contrast, the PIM-1 composite membranes have CO_2 and CH_4 permeabilities that are reduced compared to the individual membrane, while the CO_2/CH_4 selectivity is the same; given individual PIM-1 and Teflon AF1600 membranes have comparable selectivities. Similar to the single gas measurements, increasing thickness of the Teflon AF1600 layer reduces the permeability of both gases species, as the perfluoropolymer is a stronger barrier to gas transport for the PIM-1 composite membrane. The importance of these results is the difference in membrane performance under mixed gas conditions relative to that observed for single gas measurements. The impact of competitive sorption on both CO_2 and CH_4 permeability in the composite membranes clearly reduces the permselectivity, making the composite design less attractive as a potential natural gas sweetening membrane.

Table 10. Mixed gas CO_2 and CH_4 permeabilities (barrer) through 6FDA-TMPDA and PIM-1 composite membranes with Teflon AF1600, denoted by overall membrane thickness, at 35 °C.

Membrane	Thickness (μm)	CO_2	CH_4	CO_2/CH_4
6FDA-TMPDA	48	478 ± 42	23.9 ± 4	20.0
6FDA-TMPDA	50	490 ± 38	25.8 ± 2	19.0
6FDA-TMPDA	54	472 ± 41	23.5 ± 2	20.1
PIM-1	40	1927 ± 109	166 ± 11	11.6
PIM-1	43	1640 ± 110	139 ± 18	11.8
PIM-1	45	1482 ± 125	125 ± 17	11.8

Similar to the single gas composite membranes, the permeability of CO_2 and CH_4 through the 6FDA-TMPDA and PIM-1 layers of the composite membranes can be calculated through Equation (3), and the results are provided in Table 11. This assumes that the Teflon AF1600 layer permeability is unchanged from the mixed gas individual membrane performance (Table 9). For 6FDA-TMPDA the calculated CO_2 and CH_4 permeabilities are essentially the same as the individual polymer, while for PIM-1, the CO_2 permeability is higher than the individual membrane but CH_4 is essentially the same.

Table 11. Calculated permeabilities (barrer) through composite membranes' 6FDA-TMPDA and PIM-1 layers.

Membrane	CO_2	CH_4	CO_2/CH_4
6FDA-TMPDA layer	479 ± 11	22.5 ± 2	21.3
PIM-1 layer	3513 ± 153	290 ± 5	12.1

The water permeability through the composite membranes under mixed CO_2-CH_4 gas conditions as a function of water activity in the feed are provided in Figure 2 for composite PIM-1 membranes of overall thickness of 43 μm and in Figure 3 for composite 6FDA-TMPDA membranes of overall thickness of 50 μm; also included in both figures is the corresponding CO_2 permeability of the composite membrane, to indicate under which water activity conditions the composite membranes have selectivity for CO_2 over water. For both composite membranes the water permeability increases as a function of increasing water activity. This behavior has been observed for other water studies and is associated with increased water solubility at higher activities [30–32]. However, for both PIM-1 and 6FDA-TMPDA composite membranes the increase in permeability at very high water activities is substantial. High water activity may overload the ability of Teflon AF1600 to act as a barrier to water permeation, breaking down the water transport mechanism through the composite membrane and

enabling water to permeate as smaller clusters and individual molecules at high activities (Figure 1). Importantly, the PIM-1 composite membrane has water permeability lower than the CO_2 permeability for water activities below 0.2. This demonstrates that composite membranes based on PIM-1 and Teflon AF1600 can be CO_2 selective under certain water activity conditions while having higher CO_2 permselectivity than pure Teflon AF1600. The 6FDA-TMPDA composite membrane does not display this selectivity behaviour, with the membrane always having selectivity for water over CO_2.

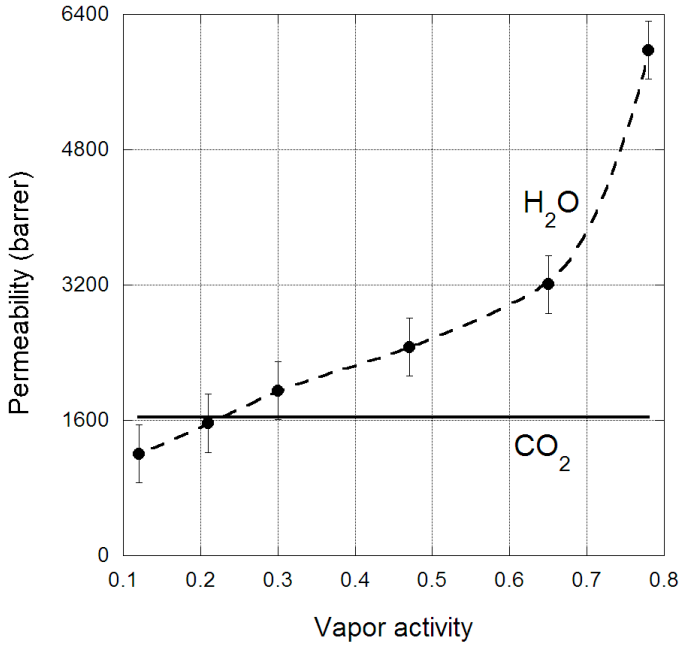

Figure 2. Permeability (barrer) of water and CO_2 through composite PIM-1 membranes under mixed gas conditions for a total thickness of 43 μm at 35 °C, for different water activities.

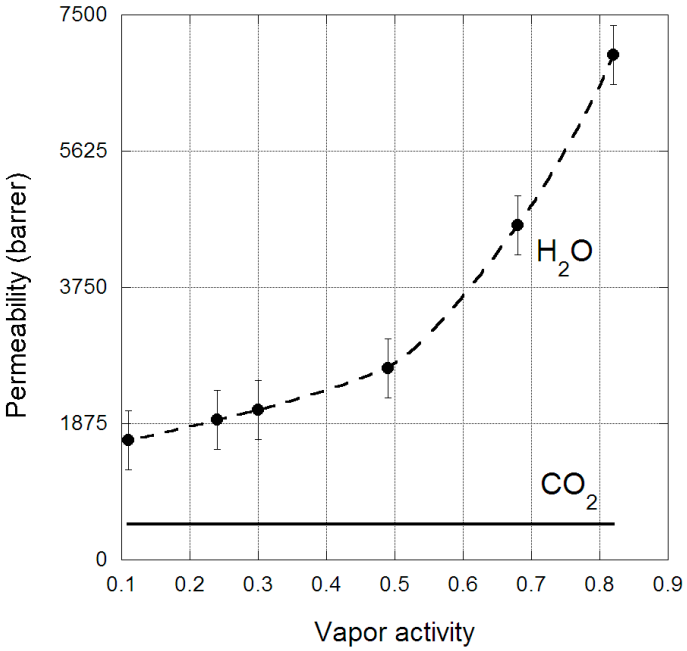

Figure 3. Permeability (barrer) of water and CO_2 through composite 6FDA-TMPDA membranes under mixed gas conditions for a total thickness at 50 μm at 35 °C, for different water activities.

4. Conclusions

Composite membranes of perfluorinated polymer Teflon AF1600 with the polyimide 6FDA-TMPDA or PIM-1 were fabricated as water vapor resistant membranes for the separation of CO_2 from CH_4. The CO_2 permeability and ideal CO_2/CH_4 selectivity of the composite membranes were clearly the function of the individual polymeric layers performance, with the permselectivity of the 6FDA-TMPDA and PIM-1 layers comparable to pure membranes of these polymers. Upon exposure to water vapor, the water permeability through the composite membranes was higher, 1740–2900 barrer, than that of the pure Teflon AF1600 membrane, 425 barrer, but retarded compared to the pure 6FDA-TMPDA and PIM-1 membranes (22,600–25,200 barrer). This reduction in water permeability was attributed to the perfluorinated polymer influencing water transport through the 6FDA-TMPDA and PIM-1 layers by inducing water clusters, which reduced the apparent water diffusivity by 64%. Furthermore, below 0.2 water activity feeds the composite PIM-1 membrane had selectivity for CO_2 over water, with higher CO_2 permselectivity than that observed for the pure Teflon AF1600 membrane. The composite 6FDA-TMPDA membrane did not demonstrate this reverse selectivity, which is partly attributed to the similar permselectivity of 6FDA-TMPDA and Teflon AF1600 under mixed gas conditions.

Author Contributions: C.A.S. conceived and designed the experiments, performed the experiments and analyzed the data. C.A.S. wrote the paper.

Acknowledgments: The author thanks Jianyong Jin at the University of Auckland for supplying the PIM-1 used in this research.

Conflicts of Interest: The author declares no conflict of interest.

References

1. Baker, R.W. Future directions of membrane gas separation technology. *Ind. Eng. Chem. Res.* **2002**, *41*, 1393–1411. [CrossRef]
2. Metz, S.J.; van de Ven, W.J.C.; Potreck, J.; Mulder, M.H.V.; Wessling, M. Transport of water vapor and inert gas mixtures through highly selective and higly selective and highly permeable polymer membranes. *J. Membr. Sci.* **2005**, *251*, 29–41. [CrossRef]
3. Bolto, B.; Hoang, M.; Xie, Z. A review of water recovery by vapour permeation through membranes. *Water Res.* **2012**, *46*, 259–266. [CrossRef] [PubMed]
4. Scholes, C.A.; Kentish, S.E.; Stevens, G.W. Effects of minor components in carbon dioxide capture using polymeric gas separation membranes. *Sep. Purif. Rev.* **2009**, *38*, 1–44. [CrossRef]
5. Lu, H.T.; Kanehashi, S.; Scholes, C.A.; Kentish, S.E. The impact of ethylene glycol and hydrogen sulfide on the performance of cellulose triacetate membranes in natural gas sweentening. *J. Membr. Sci.* **2017**, *539*, 432–440. [CrossRef]
6. Chen, G.Q.; Scholes, C.A.; Qiao, G.G.; Kentish, S.E. Water vapor permeation in polyimide membranes. *J. Membr. Sci.* **2011**, *379*, 479–487. [CrossRef]
7. Scholes, C.A.; Jin, J.; Stevens, G.W.; Kentish, S.E. Competitive permeation of gas and water vapour in high free volume polymeric membranes. *J. Polym. Sci. B Polym. Phys.* **2015**, *53*, 719–728. [CrossRef]
8. Akhtar, F.H.; Kumar, M.; Peinemann, K.-V. Pebax 1657/Graphene oxide composite membranes for improved water vapor separation. *J. Membr. Sci.* **2017**, *525*, 187–194. [CrossRef]
9. Gebben, B. A water vapor-permeable membrane from block copolymers of poly(butylene terephthalate) and polyethylene oxide. *J. Membr. Sci.* **1996**, *113*, 323–329. [CrossRef]
10. Jia, L.; Xu, X.F.; Zhang, H.J.; Xu, J.P. Permeation of nitrogen and water vapor through sulfonated polyethersulfone membrane. *J. Polym. Sci. B Polym. Phys.* **1997**, *35*, 2133–2140. [CrossRef]
11. Liu, S.; Wang, F.; Chen, T. Synthesis of poly(ether ether ketone)s with high content of sodium sulfonate groups as gas dehumidification membrane materials. *Macromol. Rapid Commun.* **2001**, *22*, 579–582. [CrossRef]
12. Sijbesma, H.; Nymeijer, K.; van Marwijk, R.; Heijboer, R.; Potreck, J.; Wessling, M. Flue gas dehydration using polymer membranes. *J. Membr. Sci.* **2008**, *313*, 263–276. [CrossRef]

13. Du, J.R.; Liu, L.; Chakma, A.; Feng, X. Using poly (n,n-dimethylaminoethyl methacrylate)/polyacrylonitrile composite membranes for gas dehydration and humidification. *Chem. Eng. Sci.* **2010**, *65*, 4672–4681. [CrossRef]
14. Metz, S.J.; van de Ven, W.J.C.; Mulder, M.H.V.; Wessling, M. Mixed gas water vapor/N2 transport in poly(ethylene oxide) poly (butylene terephthalate) block copolymers. *J. Membr. Sci.* **2005**, *266*, 51–61. [CrossRef]
15. Scholes, C.A.; Kanehashi, S.; Stevens, G.W.; Kentish, S.E. Water permeability and competitive permeation with CO_2 and CH_4 in perfluorinated polymeric membranes. *Sep. Purif. Technol.* **2015**, *147*, 203–209. [CrossRef]
16. Petropoulos, J.H. Mechanisms and theories for sorption and diffusion of gases in polymers. In *Polymeric Gas Separation*; Paul, D.R., Yampol'skii, Y.P., Eds.; CRC Press: Boca Raton, FL, USA, 1994; pp. 17–81.
17. Reijerkerk, S.R.; Knoef, M.H.; Nijmeijer, K.; Wessling, M. Poly(ethylene glycol) and poly(dimethylsiloxane): Combining their advantages into efficient CO_2 gas separation membranes. *J. Membr. Sci.* **2010**, *352*, 126–135. [CrossRef]
18. Paul, D.R.; Koros, W.J. Effect of partially immobilizing sorption on permeability and the diffusion time lag. *J. Polym. Sci. B Polym. Phys.* **1976**, *14*, 675–685. [CrossRef]
19. Koros, W.J.; Chern, R.T.; Stannett, V.; Hopfenberg, H.B. A model for permeation of mixed gases and vapors in glassy polymers. *J. Polym. Sci. B. Polym. Phys.* **1981**, *19*, 1513–1530. [CrossRef]
20. Powell, C.E.; Duthie, X.J.; Kentish, S.E.; Qiao, G.G.; Stevens, G.W. Reversible diamine cross-linking of polyamide membranes. *J. Membr. Sci.* **2007**, *291*, 199–209. [CrossRef]
21. Budd, P.M.; Elabas, B.S.; Ghanem, B.S.; Makhseed, S.; McKeown, N.B.; Msayib, K.J.; Tattershall, C.E.; Wang, D. Solution-processed, organophilic membrane derived from a polymer of intrinsic microporosity. *Adv. Mater.* **2004**, *16*, 456–459. [CrossRef]
22. Duthie, X.J.; Kentish, S.E.; Powell, C.E.; Nagai, K.; Qiao, G.G.; Stevens, G.W. Operating temperature effects on the plasticization of polyimide gas separation membranes. *J. Membr. Sci.* **2007**, *294*, 40–49. [CrossRef]
23. Tavana, H.; Petong, N.; Hennig, A.; Grundke, K.; Neuman, A.W. Contact Angles and coating film thickness. *J. Adhes.* **2005**, *81*, 29–39. [CrossRef]
24. Satilmis, B.; Budd, P.M. Base-catalysed hydrolysis of PIM-1: Amide versus carboxylate formation. *RSC Adv.* **2014**, *4*, 52189–52198. [CrossRef]
25. Hasan, R.; Scholes, C.A.; Stevens, G.W.; Kentish, S.E. Effect of hydrocarbons on the separation of carbon dioxide from methane through a polyimide gas separation membrane. *Ind. Eng. Chem. Res.* **2009**, *48*, 5415–5419. [CrossRef]
26. Thomas, S.; Pinnau, I.; Du, N.; Guiver, M.D. Hydrocarbon/hydrogen mixed-gas permeation properties of PIM-1, an amoprhous microporous spirobisindane polymer. *J. Membr. Sci.* **2009**, *338*, 1–4. [CrossRef]
27. Staiger, C.L.; Pas, S.J.; Hill, A.J.; Cornelius, C.J. Gas separation, free volume distribution, and physical aging of a highly microporous spirobisindane polymer. *Chem. Mater.* **2008**, *20*, 2606–2608. [CrossRef]
28. Scholes, C.A.; Chen, G.Q.; Stevens, G.W.; Kentish, S.E. Plasticization of ultra-thin polysulfone membranes by carbon dioxide. *J. Membr. Sci.* **2010**, *346*, 208–214. [CrossRef]
29. Cussler, E.L. *Diffusion: Mass Transfer in Fluid System*; Cambridge University Press: Cambridge, UK, 1985.
30. Reijerkerk, S.R.; Jordana, R.; Nijmeijer, K.; Wessling, M. Highly hydrophilic, rubbery membranes for CO_2 capture and dehydration of flue gas. *Int. J. Greenh. Gas Control* **2011**, *5*, 26–36. [CrossRef]
31. Potreck, J.; Nijmeijer, K.; Kosinski, T.; Wessling, M. Mixed water vapor/gas transport through the rubbery polymer PEBAX 1074. *J. Membr. Sci.* **2009**, *338*, 11–16. [CrossRef]
32. Sato, S.; Suzuki, M.; Kanehashi, S.; Nagai, K. Permeability, diffusivity, and solubility of benzene vapor and water vapor in high free volume silicon- or fluorine-containing polymer membranes. *J. Membr. Sci.* **2010**, *360*, 352–362. [CrossRef]